Structure of Quantum Wires in Au/Si(557)

I. K. Robinson,[1] P. A. Bennett,[2] and F. J. Himpsel[3]

[1]*Department of Physics, University of Illinois, Urbana, Illinois 61801*
[2]*Department of Physics and Astronomy, Arizona State University, Tempe, Arizona 85287*
[3]*Department of Physics, University of Wisconsin, Madison, Wisconsin 53706*

(Received 2 December 2001; published 15 February 2002)

The structure of the Au/Si(557) surface is determined from three-dimensional x-ray diffraction measurements, which directly mandate a single Au atom per unit cell. We use a "heavy atom" method in which the Au atom images the rest of the structure. Au is found to substitute for a row of first-layer Si atoms in the middle of the terrace, which then reconstructs by step rebonding and adatoms. The structure is consistent with the 1D metallic behavior seen by photoemission.

DOI: 10.1103/PhysRevLett.88.096104 PACS numbers: 68.43.Fg, 61.10.Eq, 68.65.La, 73.21.Hb

Quantum wires are structures that closely approximate the one-dimensional (1D) electron gas paradigm. There are many important unanswered questions about the electronic structure of 1D systems, not the least being whether spin and charge parts of the 1D electron wave function can form separate quasiparticles, leading to spatial separation of these properties, as proposed by Luttinger [1]. Intriguing electronic properties have been discovered experimentally, such as a splitting of the 1D electron band structure into two states, symmetrically positioned at the Fermi wave vector of a half-filled band [2,3]. At present there is no explanation accepted for this result, which was announced to be "spin-charge separation" [2]. Electronic band-structure calculations of sufficient sophistication should be able to resolve the issue but not without full prior knowledge of the structure at the full atomic level in 3D. Such a quantum 1D wire structure is reported here.

We report the structure of Au/Si(557), which is a surface vicinal to Si(111). Scanning tunneling microscopy (STM) has been unable to obtain the structure in sufficient detail, so we have used surface x-ray diffraction, helped by the fact that the Si(557) steps are remarkably well ordered [4]. Shibata *et al.* studied adsorption of Au on vicinal Si(111) surfaces using STM and found ordering in the steps that corresponded to (557) orientation [5], while others found (775) [6]. STM of Au/Si(557) showed double rows of protrusions with twofold periodicity along the rows [3]. However, STM cannot distinguish between Au and Si atoms, which calls for a more decisive structural technique, such as x-ray diffraction.

Other than by STM [3] and RHEED (reflection high-energy-electron diffraction) [4], there have been no previous structural studies of Au/Si(557) reported, but a number of studies of Au/Si(111). From low to high Au coverage, there are (5×2), then $(\sqrt{3} \times \sqrt{3})$, then (6×6) phases reported [7]. Atomic structures derived from x-ray diffraction are reported for each of these: the $(\sqrt{3} \times \sqrt{3})$ has a trimer of Au surrounding a threefold axis [8], while the (6×6) phase is a closer packing of such trimers [9]. The (5×2) is complicated by considerable disorder, but appears to involve substitution of rows of Au atoms into the surface layer at low-symmetry sites, combined with Si adatoms [10]; at this level it agrees with the STM observations [5,6].

The surface x-ray diffraction measurements were made at beam line X16A of the National Synchrotron Light Source (NSLS) [11]. Bending magnet radiation was monochromated to $\lambda = 1.209$ Å using double Si(111) crystals. Detector resolution was set by slits. The sample was aligned using bulk Bragg reflections, indexed according to the surface unit cell [12]. The geometry of the 557 surface dictates that this is a centered lattice containing two steps along the in-plane x direction, one Si bulk unit cell along the step edge in the y direction and 99 layers in the perpendicular z direction. Reciprocal space indices transform according to

$$\begin{pmatrix} h \\ k \\ L \end{pmatrix}_S = \frac{1}{2} \begin{pmatrix} 7 & 7 & -10 \\ -1 & 1 & 0 \\ 10 & 10 & 14 \end{pmatrix} \begin{pmatrix} h \\ k \\ l \end{pmatrix}_B , \qquad (1)$$

where "S" and "B" denote surface and bulk, respectively. Using this coordinate system, all diffraction from the simple termination of the Si(557) surface with uniformly spaced steps lies along rods with integer in-plane indices, h and k, indicating a 1×1 structure. The selection rule "$h + k$ even" follows from the centered unit cell. All rods intersect bulk Bragg peaks every 99 units along L, except where forbidden by the diamond-lattice selection rule. This identifies them all to be crystal truncation rods (CTRs) [13].

Our samples were prepared in ultrahigh vacuum by electrical heating of wafers cut to the (557) orientation. The clean Si(557) surface was found to have the 3×1 reconstruction previously reported [14]. The map of the reciprocal lattice in Fig. 1(a) shows the appearance of 1/3-order diffraction rods in addition to the CTRs passing through the bulk Si peaks. The clean structure was not analyzed, but the data appear to be consistent with the threefold step-bunched structure, suggested by STM [14].

Gold was then evaporated from a coated tungsten filament onto the samples held at 600 °C, then annealed briefly

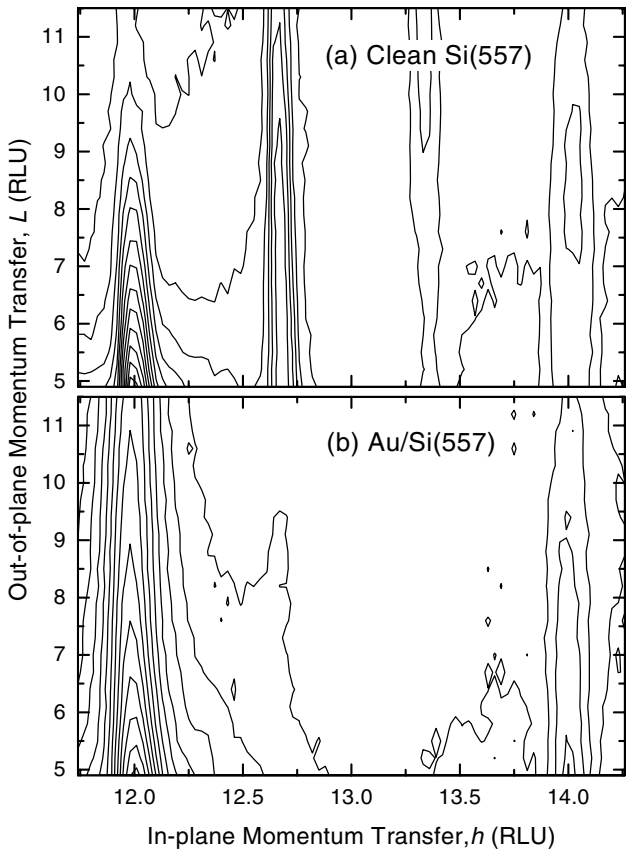

FIG. 1. Reciprocal-space maps of the intensity diffracted from the Si(557) surface. The region displayed lies between the bulk Bragg peaks at $(12, 0, 3)$ and $(14, 0, 20)$ using the surface notation defined in Eq. (1). (a) For clean Si(557), the $(12, 0, L)$ and $(14, 0, L)$ CTRs are clearly visible together with two $1/3$-order rods arising from the 3×1 reconstruction. (b) Upon dosing with Au, the reconstruction becomes lifted, and only the CTRs remain.

at 900 °C. At an estimated coverage of 0.2 monolayer, this led to a well-ordered 1×1 structure with no reconstruction. The modifications to the diffraction pattern are shown in Fig. 1(b). We looked for, but saw no sign of, the weak streak that had been reported along the step-edge y direction using low-energy electron diffraction [2,3]. The lack of ordered twofold reconstruction is consistent with the observation from STM that the double rows of bumps are randomly registered with respect to their neighbors [3]. The structure factors of the 1×1 structure were then measured by integration of rocking curves, followed by correction for the Lorentz factor, polarization, and active sample area [12]. The structure factors were averaged assuming pm symmetry to yield 349 independent measurement points, positioned along 21 crystallographically distinct CTRs, with a reproducibility of 5.3% [15].

A striking fact about the structure factor measurements is that there is very little variation throughout the whole region of the diffraction pattern measured; all the rods examined have an intensity which is almost constant in L. The numerical values vary smoothly from 40 to 60, except in the vicinity of bulk Bragg peaks where they necessarily diverge. Because Au dominates the scattering (except near Bragg peaks), this informs us immediately that the structure is very simple, with a *single* heavy atom per unit cell. This conclusion is important because it implies that the two bright rows per terrace in the STM image [3] must be due to Si and not Au atoms.

In crystallography, the situation of one heavy atom per unit cell is highly desirable because it can greatly help solve the phase problem [16]. If the heavy atom is taken to be at the crystallographic origin, the phases of all structure factors are close to zero; the Patterson (pair-correlation) function is then very similar to a Fourier electron density map of the structure. For a structure containing one Au and several Si's per unit cell, the strongest peaks (apart from the origin) correspond to Au-Si vectors; the Au is referred to as an "imaging" atom [16]. The only complication for a noncentrosymmetric structure is that *two* images of the electron density appear, the structure and an inverted *twin* image. The Patterson function is calculated directly from the data by Fourier transformation of the squares of the structure factors.

Fourier transformation of our measurements gives the Patterson map shown in Fig. 2. Considering this map to be a superposition of the $(+x, +z)$ and $(-x, -z)$ Si positions with respect to the Au at the origin, the interpretation is straightforward. To align with the bulk Si peaks far from the origin, the registry of the Au is determined to be a *substitution* for one of the Si atoms in the upper half plane of a (111) bilayer; this bulk Si lattice and its twin are indicated with different symbols on top of the map in Fig. 2. Next, the termination of the Si lattice can be read off, by noting where its continuation fails to find further peaks. This provides us with the position of the Au with respect to the step within the unit cell. Two double-height Patterson peaks (marked "A") occur where an atom in the image coincides with one from the twin. The surprise here is that the Au falls at neither the bottom nor the top edge of the step, but right in the middle of the terrace.

Finally, certain details of the atomic rearrangements can be ascertained by the presence of extra peaks in nonbulk positions. The Patterson guides us to suggest specific atomic models, which can then be tested directly with the measured structure factors. The model read off from the Patterson is shown in Figs. 3(a) and 3(b). The step-edge Si atom identified as "B" in both Figs. 2 and 3(b) has very little density in the map and is a clear candidate for omission; for this to happen, the edge could reconstruct by forming five-membered rings as shown by the dashed bonding line. The additional peak marked "C" is near the correct position for an "adatom" that could accommodate three otherwise dangling bonds on the terrace in every other unit cell (along y), thus appearing to have an occupation of 50% in the 1×1 cell. Models were built with combinations of these features and tested against the data

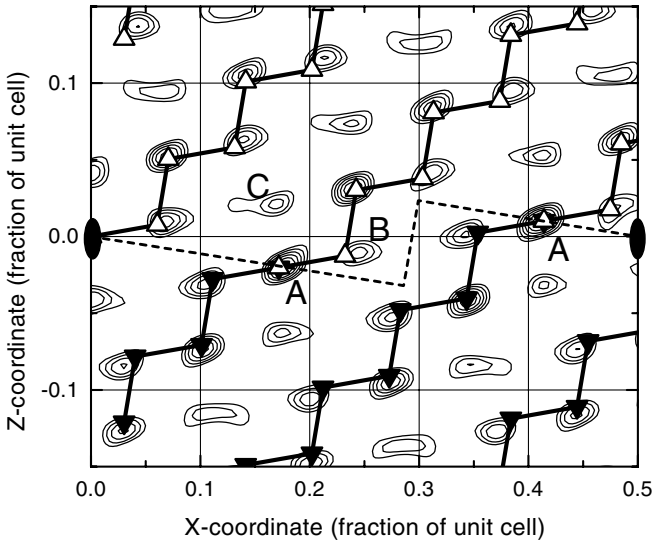

FIG. 2. Positive contours of the $y = 0$ section of the Patterson (pair correlation) function obtained directly by Fourier transformation of the CTR intensities observed for Au/Si(557). The map has twofold rotational symmetry about the origin $(x = 0, z = 0)$ (peak suppressed), and about the center $(x = \frac{1}{2}, z = 0)$, as shown by diad symbols. Because the unit cell is centered, the $y = \frac{1}{2}$ section can be obtained by a shift of $\frac{1}{2}$ in x. The interpretation drawn assumes Au at the origin and Si atoms at all the other peaks. This identifies the termination (dashed line).

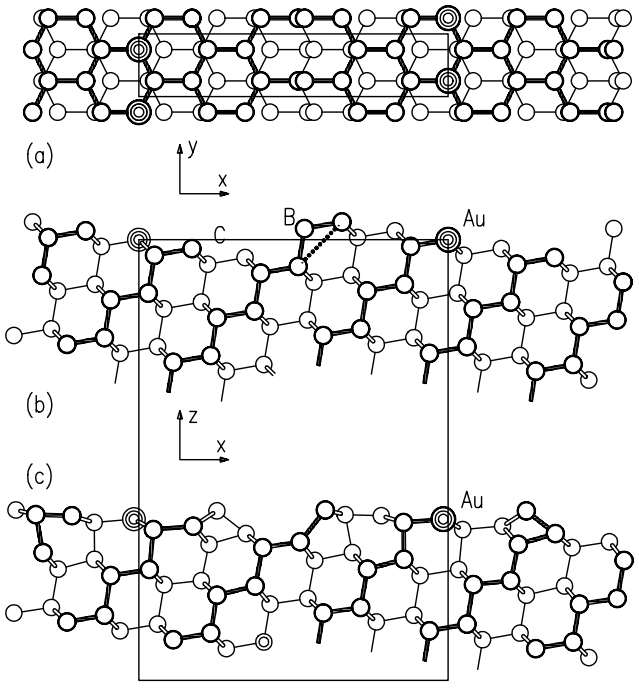

FIG. 3. Structural models of the Au/Si(557) surface. The Au atom is drawn as a triple circle. The boxes show half a unit cell in both x and z and a full cell in y, offset for clarity. (a) Top view. (b) Side view of the model read directly from the Patterson map indicating the locations of peaks "B" and "C." (c) Final model after refinement of atomic positions. Atoms and bonds closer to the viewer are drawn with heavier lines to create perspective.

using the ROD program [17] with a total of 47 free positional parameters, variable occupancy for the Au, and Debye-Waller factors (DWF) for the atoms near the step edge. Both the missing edge atom B and the adatom C were supported upon refinement of all the atomic positions in the outermost two double layers of the structure. The best agreement without the adatom was $\chi^2 = 7.5$ which dropped to $\chi^2 = 7.1$ with the adatom included [15]. The refined coordinates of the final model are shown in Fig. 3(c) and examples of the agreement with the data in Fig. 4.

The geometry in Fig. 3(c) is reasonable for a Si surface. One bond length was constrained, while the remainder (excluding the adatom) were found to be distributed with an average of 2.37 Å and a standard deviation of 0.06 Å. The bulk Si bond length is 2.35 Å. The adatom geometry showed a backbond length of 2.11 ± 0.2 Å, although this is a little unreliable because of the low occupancy. The Au occupancy of 0.73 is believed to arise from incomplete coverage or disorder in the 1×1 structure; it is probably not significant since this could have been caused by excessive postannealing during the sample preparation. The Au-Si bond lengths of 2.47 and 2.35 Å are indistinguishable from Si-Si; the Au appears to substitute in the Si lattice with relatively little strain. The DWF for the two atoms near the step edge was 3.1 ± 0.6 Å^2, suggesting some disorder there; however, attempts to fit structures with a period doubling along the step edge failed. There is a significant trend in bond *angles* that affects the overall appearance of the surface. Close to the underside of the step, the geometry is close to tetrahedral (109°), suggesting sp^3 bonding. This tends towards trigonal (120°), indicating sp^2 bonding, at the outermost end of the terrace.

The new discovery that the structure has the Au row in the *middle* of the terrace goes beyond the simple idea of step "decoration," whereby extra atoms attach themselves to a step edge to form additional bonds. Our observation of a strong gradient of strain across the terrace may be consistent with this finding. Strain relief is not needed at a step edge because the atoms on the top terrace can relax laterally (as we observe), so the Au might avoid substituting there.

Comparison of the structure with the STM images [3] is revealing. The three prominent elevated features on the surface in Fig. 3 are the Au row, the adatom row, and the step edge. The distances between these are Au adatom 5.2 Å, adatom edge 7.0 Å, and edge Au 7.3 Å. The two rows seen in the STM images are 7.3 ± 0.7 Å apart [3]. While we cannot make a definitive assignment of the STM separation based on distance alone, we believe this represents the adatom-edge spacing because it can explain the doubled modulation along y of both rows: the adatoms are present in every other unit cell, while the step edge can adopt a height modulation that couples to the adatoms.

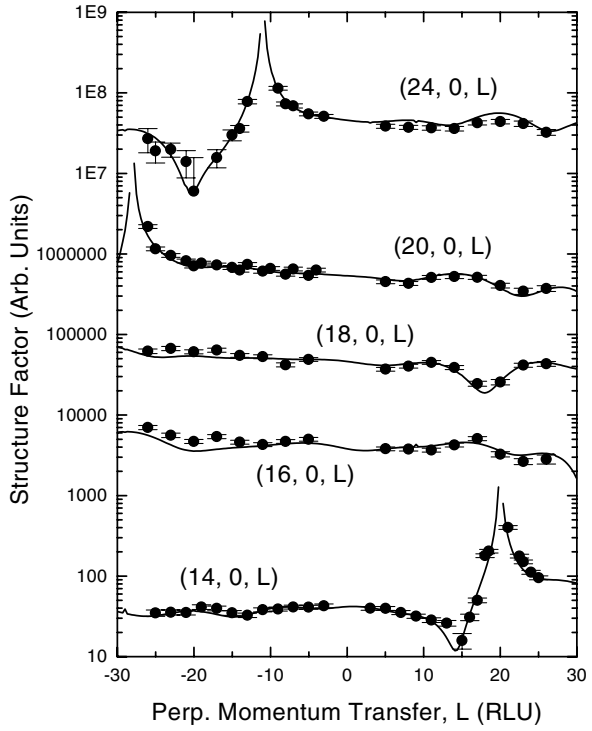

FIG. 4. Representative measurements of x-ray structure factors of Au/Si(557) together with the calculated curves from the best model. The curves are offset by factors of 10 on the logarithmic scale for clarity.

Although this height modulation is not observed directly here, it is consistent with the enhanced DWF of the step edge. We conclude that the prominent features seen in STM are due to Si and not Au.

The finding that the gold row does not exhibit a Peierls distortion (within the limit of our experiment) is consistent with the metallic behavior seen in photoemission [2,3]. The anchoring of the metal chain to the rigid silicon lattice apparently suppresses the Peierls transition that would lead to an insulator. This opens further possibilities for studying exotic electron liquids in one dimension, such as the Luttinger liquid [1].

We conclude by noting that this is a remarkably simple structure, considerably simpler than any of the known structures of Au/Si(111) [6–10] or Au/Si(100) [18]. The solution of this structure should make resolution of its electronic band structure more tractable by theory. In fact, the observed band structure of Au/Si(557) is also much simpler than the (5×2) of Au/Si(111) [3], which is another chain structure [10]. Total energy and band calculations have already begun [19] and have found independently that the position of the Au chain in the middle of the terrace is indeed energetically favorable.

The NSLS facility is supported under DOE Contracts No. DEAC02-98CH10886 and No. DEFG02-91ER45439. This research was supported by the National Science Foundation under Contracts No. DMR 98-76610, No. DMR 99-81779, No. DMR 96-32635, and No. DMR 98-15416.

[1] J. M. Luttinger, J. Math. Phys. (N.Y.) **4**, 1154–1162 (1963).
[2] P. Segovia, D. Purdie, M. Hengsberger, and Y. Baer, Nature (London) **402**, 504–507 (1999).
[3] R. Losio, K. N. Altmann, A. Kirakosian, J. L. Lin, D. Y. Petrovykh, and F. J. Himpsel, Phys. Rev. Lett. **86**, 4632–4635 (2001); K. N. Altmann *et al.*, Phys. Rev. B **64**, 035406 (2001).
[4] M. Jalochowski, M. Strozak, and R. Zdyb, Surf. Sci. **375**, 203 (1997).
[5] M. Shibata, I. Sumita, and M. Nakajima, Phys. Rev. B **57**, 1626 (1998).
[6] L. Seehofer, S. Huhs, G. Falkenberg, and R. L. Johnson, Surf. Sci. **329**, 157–166 (1995).
[7] D. Grozea, E. Bengu, and L. D. Marks, Surf. Sci. **461**, 23–30 (2000).
[8] D. Dornisch *et al.*, Phys. Rev. B **44**, 11 221 (1991).
[9] D. Grozea *et al.*, Surf. Sci. **418**, 32–45 (1998).
[10] R. Feidenhans'l *et al.,* in *Kinetics of Ordering and Growth at Surfaces,* edited by M. G. Lagally (Plenum Press, New York, 1990); C. Schamper *et al.*, Phys. Rev. B **43**, 12 130 (1991); L. D. Marks and R. Plass, Phys. Rev. Lett. **75**, 2172 (1995).
[11] P. H. Fuoss and I. K. Robinson, Nucl. Instrum. Methods Phys. Res., Sect. A **222**, 171 (1984).
[12] I. K. Robinson and D. J. Tweet, Rep. Prog. Phys. **55**, 599–651 (1992).
[13] I. K. Robinson, Phys. Rev. B **33**, 3830 (1986).
[14] A. Kirakosian, R. Bennewitz, J. N. Crain, T. Fauster, J. L. Lin, D. Y. Petrovykh, and F. J. Himpsel, Appl. Phys. Lett. **79**, 1608 (2001).
[15] Because they are based on the symmetry equivalents and the *pm* symmetry is rather low, the systematic errors are probably underestimated. Errors of 10% are more usual for this instrument, which would reduce χ^2 by a factor of 4.
[16] H. B. Dyer, Acta Crystallogr. **4**, 42 (1951).
[17] E. Vlieg, J. Appl. Crystallogr. **33**, 401 (2000).
[18] X. F. Lin, K. J. Wan, J. C. Glueckstein, and J. Nogami, Phys. Rev. B **47**, 3671 (1993).
[19] D. Sanchez-Portal and S. C. Erwin (private communication).